ESTIMATION OF RELATIVE PEREMABILITY OF SINGLE FRACTURE BY USING MULTI-PHASE LATTICE BOLTZMANN METHOD

T. AKAI[1], H. OKABE[1], S. MURATA[2]
[1]Japan Oil, Gas and Metals National Corporation (JOGMEC), Chiba, Japan
[2]Graduate School of Engineering, Kyoto University, Kyoto, Japan

ABSTRACT: For the successful and efficient development of a fractured oil/gas reservoir, it is important to estimate multi-phase fluid flow behavior in the fracture. In many cases, the fluid flow in the fracture has been studied by the simplified model as parallel smooth plates. Therefore, the anisotropy of the fluid flow behavior inside the fracture has not been estimated accurately. Moreover, it is not well understood how the wettability of the fracture surfaces, the interfacial tension between water and oil, and the geometries of the fracture surfaces affect the multi-phase flow behavior even in the single fracture. In this study, in order to understand these phenomena, we investigated the multi-phase flow behavior in the single fracture model and try to determine the fracture relative permeability of oil and water by performing water flooding simulations using Multi-phase Lattice Boltzmann Method. By this study, the effects of the wettability and the interfacial tension on the multi-phase flow behavior and the relative permeability in the fracture have been clarified.

INTRODUCTION

In the oil/gas exploration and production business, production from the fractured reservoirs has been increasing. McNaughton and Grab estimated that ultimate recovery from currently producing fractured reservoirs will be exceeded 40 billion stock tank barrels of oil[1)]. However, in spite of the importance of fractured reservoirs, many technical problems are still unsolved. The problems can be classified into three groups. The first is the detection and quantification of fracture distribution, the second is the evaluation of fracture communication and the third is the understanding of multi-phase flow phenomena in a fracture. In this paper, we focus on the understanding of multi-phase fluid flow in the fracture.

Generally, the fracture permeability is estimated by the cubic law, that is, the volumetric flow rate in a fracture is directly proportional to the cubic of its aperture. This law is valid for the laminar flow between two perfectly smooth parallel plates. However, the fractures have complicated rough surfaces. This makes the fluid flow through them anisotropic and their permeability deviate from the cubic law. Fig.1 shows the single phase fluid flow simulation result carried out by Watanabe, et al[2)]. They conducted single phase fluid flow simulations by solving local cubic law to a fracture model constructed by X-ray CT image. In this figure, an anisotropic and preferential flow path can be observed and the evaluated permeability was deviated from the cubic law.

In the case of multi-phase flow, the two straight lines satisfying the relation of $k_{r,nw}+k_{r,w} = 1$ as shown in Fig.2 have been widely used for the fracture relative permeability curves based on the experimental works by Romm (1966), where $k_{r,nw}$ and $k_{r,w}$ are the relative permeability of non-wetting phase and wetting phase respectively. This type of relative permeability curves physically means that each phase flows in its own flow path without interference. But, some theoretical or experimental works and some numerical simulations to the two-phase flow in a single fracture have shown that each phase flows with strong phase interference[3-6)]. However, these works are not sufficient to understand the phase interference flow behavior for the correct estimation of the fracture relative permeability. Therefore, additional detail research on the multi-phase flow in a single fracture must be performed.

In this study, we try to simulate and to estimate the relative permeability to the single fracture model having complex surface geometry by performing two-phase flow simulations using the Lattice Boltzmann method (LBM). Moreover, we investigate the effects of the wettability and the interfacial tension on the multi-phase flow behavior and the relative permeability by the Multi-phase LBM flow simulations.

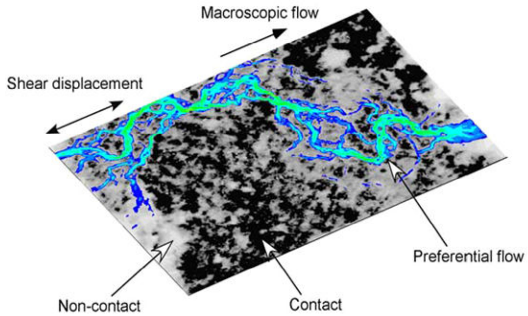

Figure 1 The result of single phase fluid flow simulation by Watanabe et al. (2010)

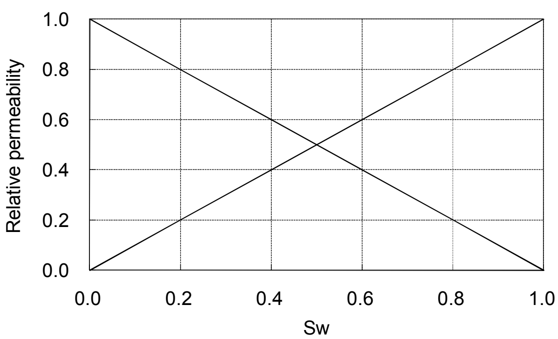

Figure.2 The fracture relative permeability curves based on experimental works by Romm. (1966)

CONSTRUCTION OF MULTI-PHASE LATTICE BOLTZMANN MODEL

Multi-phase LBM

The Lattice Boltzmann Method (LBM) is based on cellular automata, which describes a complex system by the interaction of a massive number of cells following simple local rules[7)]. While other methods, such as the FEM or the FDM, discretize the model and the governing equations, the LBM method recovers the governing equation from the rule in the discrete model.

In order to simulate the immiscible two-phase flow of oil and water, the Boltzmann equation for the colored particles, red (oil) and blue (water), was used in this study. It is given by the following equation.

$$f_i^k\left(\mathbf{x}+\mathbf{c}_i\Delta t, t+\Delta t\right)=f_i^k\left(\mathbf{x},t\right)+\Omega_i^k\left(\mathbf{x},t\right) \tag{1}$$

Where $f_i^k(\boldsymbol{x},t)$ and $\Omega_i^k(\mathbf{x},t)$ are the particle distribution function and the collision function respectively. They are defined to every kind of particle k, red and blue, and to every direction of particle motion i at the position $\mathbf{x}$ and time t. In Equation (1), $\boldsymbol{c}_i$ is the particle velocity in i direction on the lattice, and Δt is the time step during which the particles travel one lattice spacing. The particle velocity vectors on the D3Q15 (3D-LBM with 15 velocities) lattice used in this study is given by

$$\mathbf{c}=\begin{bmatrix} 0 & 1 & 0 & 0 & -1 & 0 & 0 & 1 & -1 & 1 & 1 & -1 & 1 & -1 & -1 \\ 0 & 0 & 1 & 0 & 0 & -1 & 0 & 1 & 1 & -1 & 1 & -1 & -1 & 1 & -1 \\ 0 & 0 & 0 & 1 & 0 & 0 & -1 & 1 & 1 & 1 & -1 & -1 & -1 & -1 & 1 \end{bmatrix} \tag{2}$$

The collision function is decomposed into two terms as Equation (3).

$$\Omega_i^k\left(\mathbf{x},t\right)=\left(\Omega_i^k\left(\mathbf{x},t\right)\right)^A+\left(\Omega_i^k\left(\mathbf{x},t\right)\right)^B \tag{3}$$

The first term of the right side of Equation (3) represents the relaxation from the collision perturbing condition to the local equilibrium condition. This term determines the effect of fluid viscosity in the LBM simulation. The second term represents the surface tension between the two kinds of immiscible fluid.

The first term of the collision function is defined as Equation (4) applying BGK (Bhatnagar-Gross-Krook) collision operator.

$$\left(\Omega_i^k\left(\mathbf{x},t\right)\right)^A=-\frac{1}{\tau^k}\left(f_i^k\left(\mathbf{x},t\right)-f_i^{k(eq)}\left(\mathbf{x},t\right)\right) \tag{4}$$

Where τ^k is the relaxation time to the local equilibrium condition after collision, and $f_i^{k(eq)}$ is the local equilibrium particle distribution function. In this study, in order to get the numerical stability, the value of τ^k is set to 1. On the other hand, the second term of the collision function is defined by Equation (5) applying the interfacial tension model proposed by Grunau *et al*[8)].

$$\left(\Omega_i^k\left(\mathbf{x},t\right)\right)^B=A\left|\mathbf{F}\right|\left(\frac{\left(\mathbf{c}_i\cdot\mathbf{F}\right)^2}{\left|\mathbf{c}_i\right|^2\left|\mathbf{F}\right|^2}-K\right) \tag{5}$$

Where A is the coefficient which controls the magnitude of interfacial tension, and K is the coefficient determined from the mass conservation depending on the lattice model. In this study, A is set to 1.0x10^{-3} for the base case of interfacial tension. K is 1/3 for the 3D15Q lattice model. $\mathbf{F}$ is a function called local color gradient. It is defined by Equation (6).

$$\mathbf{F}(\mathbf{x},t)=\sum_i\mathbf{c}_i\left(\rho_r(\mathbf{x}+\mathbf{c}_i\Delta t,t)-\rho_b(\mathbf{x}+\mathbf{c}_i\Delta t,t)\right) \tag{6}$$

Where ρ_r and ρ_b are the density of red fluid and blue fluid respectively. This function has a contribution at the interface of immiscible fluids.

Verification of simulation model

The change of contact angle depending on the wettability and the Young-Laplace relation were simulated in order to confirm the validity of the interfacial tension model used in the multi-phase LBM.

Wettability is an index how the solid surface has a tendency to be wet with the contacting fluid. It is estimated by the contact angle, θ_c, of a droplet on the solid surface. When a droplet of oil contacts a rock surface in water and the contact angle measured through the oil is less than 90 degrees, the rock surface must be oil wet. Conversely, when it is more than 90 degrees, the rock surface must be water wet. Moreover, when it is just 90 degrees, the rock surface must be neutral wet.

Supposing the following relations among the interfacial tensions between the rock surface and the oil, $\gamma_{s\text{-}o}$, the oil and the water, $\gamma_{o\text{-}w}$ and the rock surface and the water, $\gamma_{s\text{-}w}$,

$$\gamma_{s-o} = \lambda \gamma_{o-w} \tag{7}$$

$$\gamma_{s-w} = (1-\lambda)\gamma_{o-w} \tag{8}$$

Where λ is the scaling parameter ranging from 0.0 to 1.0. The contact angle can be obtained from the Young's equation as

$$\cos\theta_c = 1 - 2\lambda \tag{9}$$

Therefore, any contact angle of rock surface can be realized by setting λ according the Equation (9).

Then, the contact angle of an oil droplet on a flat rock surface in water was simulated to the case of the perfectly water wet, λ=1.0, the neutral wet, λ=0.5, and the perfectly oil wet, λ=0.0. The results of the simulation are shown in Fig.3. In the case of the perfectly water wet, the oil droplet changed its shape from the initial condition in Fig. 3(a) to be a sphere as shown in Fig.3(b). In the case of the neutral wet, the oil droplet changed its shape to be a semi-sphere as shown in Fig.3(c). In the case of the perfectly oil wet, the oil droplet spread itself on the rock surface as shown in Fig.3(d). From these results, we can recognized that the contact angles are well simulated, although it looks larger than 0 degree in the case of the perfectly oil wet.

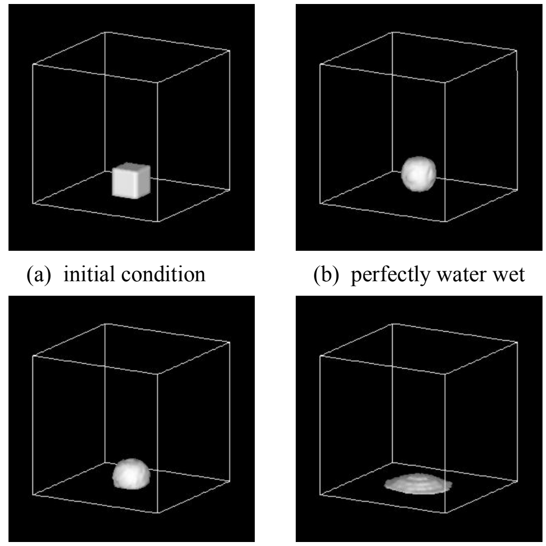

(a) initial condition (b) perfectly water wet

(c) neutral wet (d) perfectly oil wet

Figure 3 The realization of wettability condition of rock surface in the LBM

Next, the Young-Laplace relation described by Equation (10) must be satisfied when a droplet of one phase exists in another immiscible phase under the static condition.

$$\Delta p = p_{in} - p_{out} = \frac{2\gamma}{R} \tag{10}$$

Where p_{in} is the inside phase pressure of the droplet; p_{out} is the outside phase pressure of the droplet; γ is the interfacial tension, R is the radius of the droplet.

Then, a square oil droplet was put in the water, and the pressure difference between the oil and the water, Δp, and the radius of the oil droplet, R, was evaluated under the static equilibrium condition. The relation between the Δp and the reciprocal of the radius, $1/R$, was plotted by changing the volume of the square oil droplet. The simulation was carried out to the two cases of interfacial tension by setting the coefficient of A=1.0x10^{-3} and 0.5x10^{-3}. They are the base case of interfacial tension and the half of the base case. The result of the plot is shown in **Fig.4**. From this figure, it can be recognized that the Δp is directly proportional to the $1/R$, and the Young-Laplace relation is satisfied.

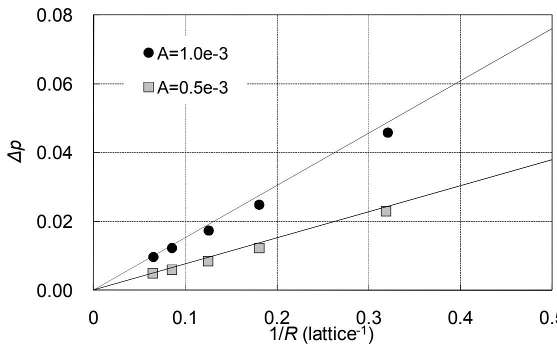

Figure 4 The realization of Young-Laplace relation the pressure difference between oil and water and the reciprocal of the radius of the oil droplet, R.

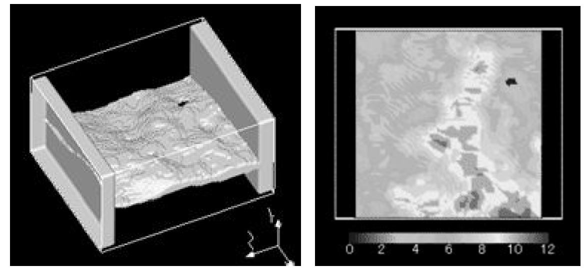

(a) bird view (b) aperture distribution

Figure 5 The single fracture model used for the multi-phase simulation.

Table 1 The description of the fracture model used in the study.

Lattice interval	0.05 (mm/lattice)
Size of Fracture area	120 x 100 (lattice)
Contact ratio	0.8 (%)
Max. aperture	12 (lattice)
Mean aperture	4.2 (lattice)

WATER FLOODING SIMULATION

Single fracture model used for the simulation

It has been shown that the topography of a fracture surface is a self-affine fractal and the power spectral density function of the fracture surface profile, $G(f)$, shows a decaying power law that can be described as

$$G(f) = Cf^{-(5-2D)} \tag{11}$$

Where D is the fractal dimension; C is a constant; f is the spatial frequency[9,10]. The two meeting surfaces of a single fracture correlate each other in the lower spatial frequency band and do not correlate in the higher spatial frequency band. The fracture surfaces interlock and the aperture distribution is generated by this frequency dependent correlation.

In order to generate such a fracture numerically, we used the Glover's method[11]. The fractal dimension and the roughness of the generated fracture surfaces are set by changing the slope and the intersection of the decaying power law respectively. We generated a square single fracture model of 1024 lattices in side length and 64 lattices in thickness. Then, a single fracture model of 100 lattices in side length and 64 lattices in thickness was cut out and the 10 lattices in length and 64 lattices in thickness of fluid buffer regions were added to the both sides of inlet and outlet. The single fracture model is shown in Fig.5 and its descriptions are listed in Table 1.

Relative permeability estimation of a single fracture

By conducting multi-phase LBM simulation to the fracture model, the relative permeability of the single fracture model was estimated from the average flux of each phase and the water saturation. In this simulation, the fracture was perfectly saturated with water at first, and then oil was injected under the constant pressure gradient until the irreducible water saturation was accomplished. After that, the water flooding was carried out. The simulation conditions are summarized in Table 2.

The snapshots during the simulation are show in Fig.6. At first, water invades even in the small aperture regions avoiding the oil saturated large aperture regions. Then, as result of water breakthrough, two isolated oil islands are formed (20,000 steps). After that, one of them is swept by the injected water, but the other is remained.

Oil and water relative permeability curves concaving downward are obtained as shown in Fig.7. It can be recognized that the relative permeability curves of a single fracture are not straight lines satisfying the relation of $k_{r,nw}+k_{r,w} = 1$. This is probably because the each phase of fluid flows avoiding or pushing each other in the complex aperture distribution of the fracture, and the flow path consequently becomes as tortuous as the porous reservoir rocks.

Table 2 The simulation condition.

Density	Water	1.0×10^3kg/m^3
	Oil	0.9×10^3kg/m^3
Viscosity	Water	1.0×10^{-3}Pa・s
	Oil	4.5×10^{-3}Pa・s
Wettability		Perfectly water wet
Interfacial tension		A=1.0×10^{-3} (Base case)
Boundary condition		Constant pressure boundary

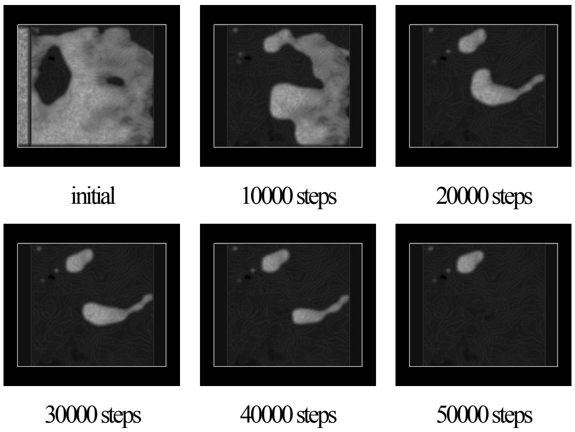

Figure 6 The change of oil saturation during the water flooding. (Gray color represents oil, block color represents water.)

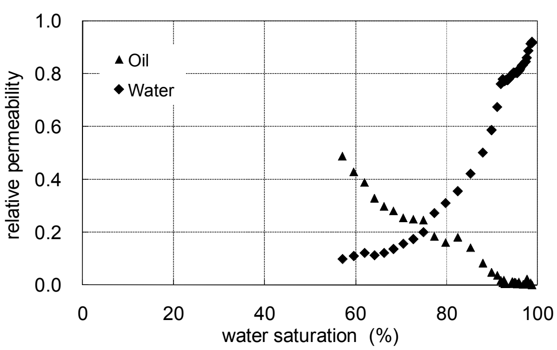

Figure 7 The fracture relative permeability curves of oil and water obtained from the water flooding simulation.

Effect of wettability on relative permeability

Water flooding simulations were performed to the perfectly water wet, the neutral wet, and the perfectly oil wet to the same single fracture model as mentioned above. However, the viscosity ratio was set to one in order to diminish the effect of viscosity. The initial water saturation is 57.2% to the water wet, 42.6% to the neutral wet, and 20.7% to the oil wet (**Fig.8**). From this initial water saturation condition, water was injected into the fracture under the constant pressure gradient.

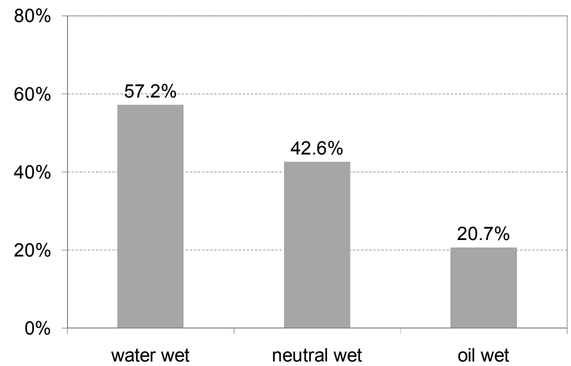

Figure 8 The initial water saturation of each wettability condition. (Before water flooding)

The change of the oil saturation is shown in **Fig.9** to each case of the wettability in the progress of time step. In the case of the perfectly water wet, it is shown in Fig.9(a), the aspect of the flooding is the same as above mentioned. The residual oil saturation is 1.5%. In the case of the neutral wet, it is shown in Fig.9(b), the almost all of oil is flooded out continuously without forming the independent oil islands. The residual oil saturation is 0.74%. In the case of the perfectly oil wet, it is shown in Fig.9(c), the water invades selectively the large aperture regions. Two flow paths are formed as the result of avoiding the surface contact region, and the two flow paths surround the small aperture region around the surface contact region. The oil in that small aperture region is left finally. The residual oil saturation is 5.7% that is the highest among the three cases of wettability condition (Fig.10).

The relative permeability curves are shown in Fig.11 to each case of the wettability condition. In the case of the perfectly water wet, the water relative permeability is difficult to increase during the small water saturation, because the water flows by avoiding the oil occupying large aperture region. But it rapidly increases with the increase in the water saturation, as the water flows through almost the whole fracture. Consequently, the water relative permeability curve concaves downward. In the case of the neutral wet, the both relative permeability curves of oil and water become almost straight line. This is because the each phase of the fluid can flow without capillary force. In the case of the perfectly oil wet, the relative permeability concaving upward is obtained. This is because the water invades selectively the large aperture regions at first and then it spreads into the small aperture regions. The flow rate of the water decreases as the result.

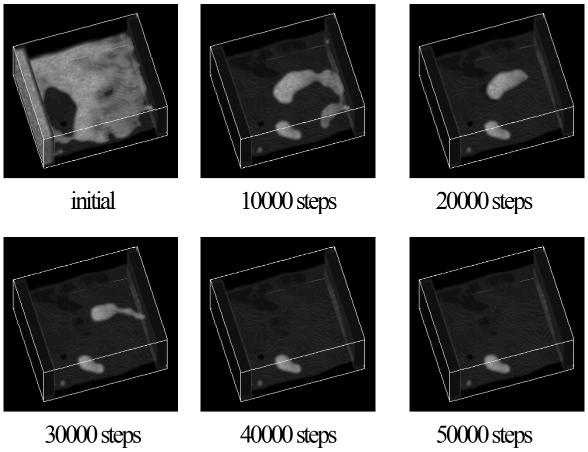

(a) perfectly water wet

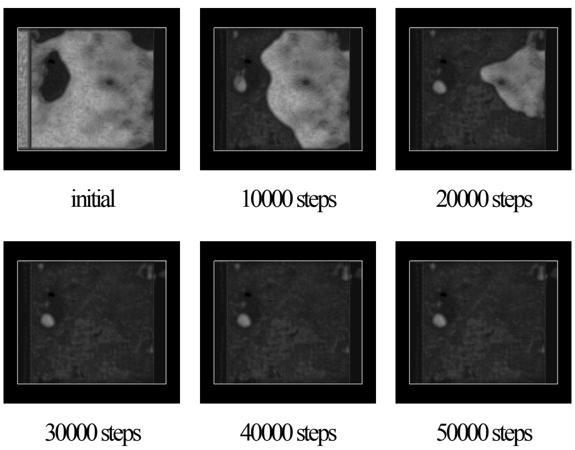

(b) neutral wet

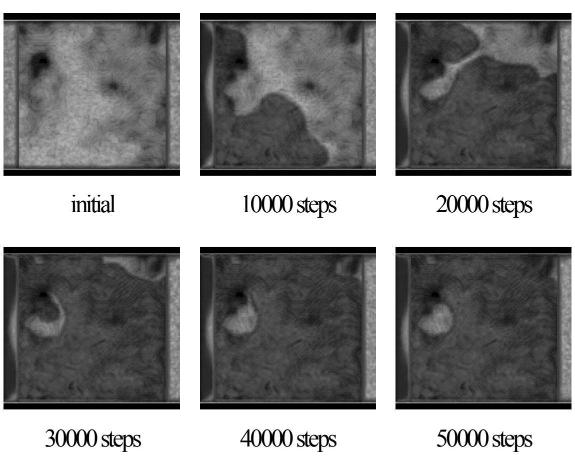

(c) perfectly oil wet

Figure 9 The change of oil saturation during the water flooding. (Gray color represents oil, block color represents water.)

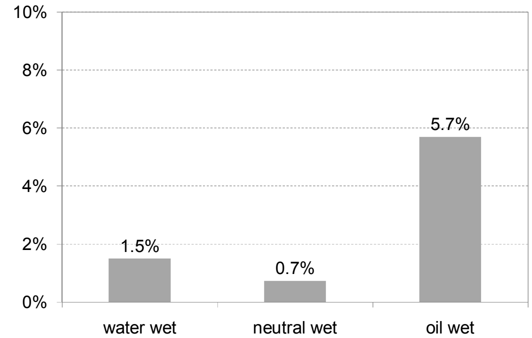

Figure 10 The residual oil saturation of each wettability condition. (After water flooding)

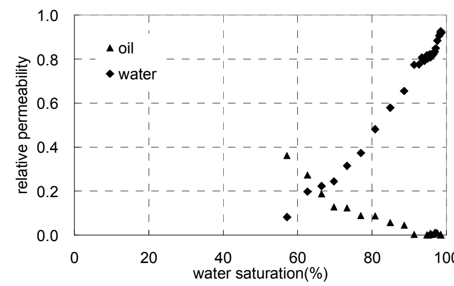

(a) perfectly water wet

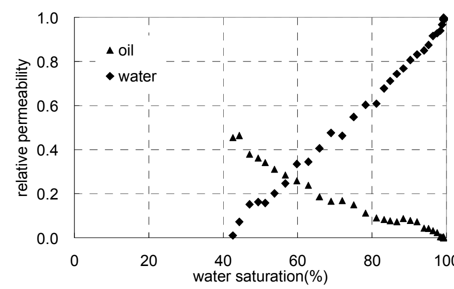

(b) neutral wet

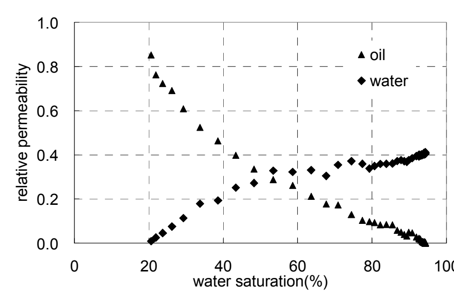

(c) perfectly oil wet

Figure 11 The relative permeability curves of each wettability condition.

Effect of interfacial tension on relative permeability

The effect of the interfacial tension on the relative permeability was secondly investigated. We set the value of interfacial tension controlling coefficient, *A*, 1/10 of the base case, and performed the water flooding simulation to the cases of perfectly water wet and the perfectly oil wet. The pressure gradient and viscosity ratio are the same with the previous simulations.

Although the flow pattern of the both cases of the wettability condition is almost the same with the base case of the interfacial tension, the formed oil islands become smaller in the case of the perfectly water wet and the water invades into the smaller aperture regions in the case of the perfectly oil wet by reducing the interfacial tension. The residual oil saturation decreases in the both cases of the wettability. The residual oil saturation is 0.04% to the perfectly water wet and 4.2% to the perfectly oil wet.

The relative permeability curves are shown in **Fig.12** to each case of the wettability condition. In the both cases of wettability condition, the relative permeability curves approach the straight line which is shown in **Fig.2**. This is probably because the capillary effect becomes small and the flow behavior of the both fluids becomes independent of the aperture distribution.

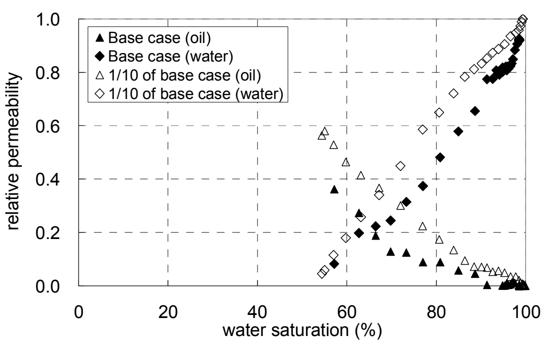

(a) perfectly water wet

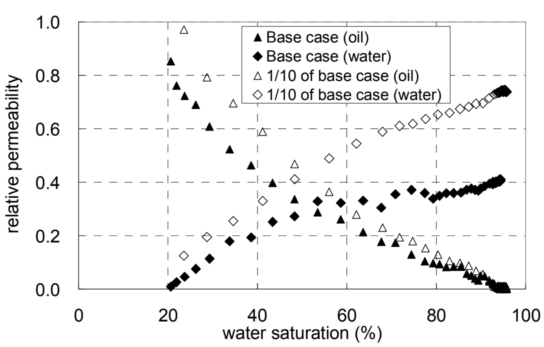

(b) perfectly oil wet

Figure 12 The change of relative permeability curves due to the decrease of interfacial tension.

CONCLUSION

Multi-phase flow behavior is simulated by the LBM used in the study, and the relative permeability of oil and water for the single fracture is estimated.

As a result of the water flooding simulation in the fracture having a complex topology of surface, residual oil is observed clearly.

In the case of perfectly water wet surface, the residual oil is remained in isolated droplet shape from the flow path of water phase.

In the case of perfectly oil wet surface, the residual oil is remained at the small aperture region around the surface contact region.

The fracture relative permeability curves of oil and water are not the straight lines but the curves whose shape depend on the wettability of the fracture surface and interfacial tension between oil and water.

The water relative permeability curve concaves downward when the wettability is perfectly water wet , and it concaves upward when the wettability is perfectly oil wet.

The relative permeability curves of oil and water approach a straight line regardless of the wettability when the interfacial tension between oil and water is reduced.

ACKNOWLEDGMENT

We would like to appreciate JOGMEC's support and Dr. Murata's technical supervision to this study and the permission to submit this paper.

REFERENCES

Roberto Aguilera (1980): Naturally Fractured Reservoirs, pp.1-2,

N. Watanabe, Y. Osaki, Y.Thuchiya, T. Tamagawa, N. Hirano, H. Okabe, N. Thuchiya (2010), Analysis of fracture flow by numerical modeling coupled with X-ray CT computed tomography, *Japan Geoscience Union Meeting* 23-28 May 2010 (Japanese)

Rossen, W. R., and Kumar, A. T. K., (1992), Single- and two-phase flow in natural fractures, *Proc. of the 67th SPE ATC*, paper SPE-24195.

Persoff, P., and Pruess, K., (1995), Two-phase flow visualization and relative permeability measurement in natural rough-walled rock fractures, Water Resour. Res., 31(5), p. 1175-1186.

Iwai, T., and Tosaka, H., (2003), Laboratory measurement of relative permeability of air-water two-phase flow in a single fracture (in Japanese), Shigen-to-Sozai, 119., p. 593-598.

Speyer, N., Li, K., and Horne, R., (2007), Experimental measurement of two-phase relative permeability in vertical fractures, *Proc. of 32nd workshop on geothermal reservoir engineering Stanford University*, SGP-TR-183.

Youngseuk Keehm (2003) :Computational Rock Physics: Tranport Properties in Porous Media and Applications, pp.12-21.

Grunau, D., Chen, S. and Eggert, K., (1993), A lattice Boltzmann model for multiphase fluid flows, Phys. Fluids A, 5(10), p. 2557-2562.

Brown, S. R., and Scholz ,C. H., (1985), Broad bandwidth study of the topography of natural rock surfaces. *J. Geophys*. Res., 90, p. 12575-12582.

Power, W. L., and Tullis, T. E., (1991), Euclidean and fractal models for the description of rock surface roughness, *J. Geophys*. Res., 96, p. 415-424.

Glover, P. W., J., Matsuki, K., Hikima, R. and Hayashi, K., (1997), Fluid flow in fractally rough synthetic fractures, *J. Geophys.* Res, Lett., 24, p. 1803-1806.